Transcription factor induction of human oligodendrocyte progenitor fate and differentiation

Jing Wang, Suyog U. Pol, Alexa K. Haberman, Chunming Wang, Melanie A. O'Bara, and Fraser J. Sim[1]

Department of Pharmacology and Toxicology, School of Medicine and Biomedical Sciences, University at Buffalo, Buffalo, NY 14214

Edited by Ben A. Barres, Stanford University School of Medicine, Stanford, CA, and approved June 3, 2014 (received for review May 9, 2014)

Human oligodendrocyte progenitor cell (OPC) specification and differentiation occurs slowly and limits the potential for cell-based treatment of demyelinating disease. In this study, using FACS-based isolation and microarray analysis, we identified a set of transcription factors expressed by human primary CD140a$^+$O4$^+$ OPCs relative to CD133$^+$CD140a$^-$ neural stem/progenitor cells (NPCs). Among these, lentiviral overexpression of transcription factors ASCL1, SOX10, and NKX2.2 in NPCs was sufficient to induce Sox10 enhancer activity, OPC mRNA, and protein expression consistent with OPC fate; however, unlike ASCL1 and NKX2.2, only the transcriptome of SOX10-infected NPCs was induced to a human OPC gene expression signature. Furthermore, only SOX10 promoted oligodendrocyte commitment, and did so at quantitatively equivalent levels to native OPCs. In xenografts of *shiverer/rag2* animals, SOX10 increased the rate of mature oligodendrocyte differentiation and axon ensheathment. Thus, SOX10 appears to be the principle and rate-limiting regulator of myelinogenic fate from human NPCs.

neural precursor cell | transplantation | reprogramming

The loss of oligodendrocytes and myelin in the central nervous system occurs in both pediatric and adult disease (1). Demyelination directly contributes to loss of axonal signal transduction, and leads to irreversible axonal atrophy and neurodegeneration. Myelin replacement, or remyelination, may be therapeutically achieved by stimulation of endogenous regeneration or transplantation of myelinogenic cell populations. Although remyelination is efficient in animal models of demyelination, in human lesions endogenous progenitors appear to be limited in both their mitotic competence and differentiation (2). The transplantation of human oligodendrocyte progenitor cells (OPCs) has shown that exogenous human cells are capable of myelinating large regions of white matter and, in so doing, restore axonal conduction and prevent the early demise of *shiverer* hypomyelinating mice (3).

Human OPCs have been directly isolated from brain tissue using a variety of surface antigen-based approaches (3–6). In these studies, the rate of donor-derived myelination was dependent on both developmental stage and purity of the cell population. However, as human OPCs cannot be readily expanded following isolation, various approaches have been used to specify OPC fate from embryonic stem cells (7, 8). Although these procedures are able to generate enriched cultures of antigenically defined OPCs, specification of platelet-derived growth factor α receptor (PDGFαR)-expressing OPCs from OLIG2$^+$ neural stem/progenitor cells (NPCs) requires more than 8 wk in culture, and the resulting cells initiate myelination at a significantly slower rate than native PDGFαR/CD140a-defined OPCs directly isolated from fetal human brain (5, 9). More recently, human induced pluripotent stem cells (iPSCs) have been directed to OPC fate by similar exogenous factors. Although these cells are capable of expansive myelination in *shiverer*, myelination occurs more slowly than in native PDGFαR+ OPCs, and the procedure requires several months in vitro (10). The rate-limiting step appears to be OPC specification, because, unlike rodent NPCs, human primary NPCs do not readily differentiate as OPCs or oligodendrocytes in vitro (11, 12).

In this study, we sought to identify and characterize the rate-limiting transcription factors (TFs) that govern human OPC fate. Although several TFs are known to be necessary for oligodendrocyte fate and differentiation (reviewed in ref. 13), much less is known about those that act during OPC specification. Given the species differences in OPC gene expression (14), it is likely that the role of these TFs is subtly different in human cells. To select instructive TFs in an unbiased manner, we performed microarray analysis on antigenically defined human progenitors (15, 16). We compared the transcriptional profile of CD140a and O4-defined OPCs with that of CD133$^+$CD140a$^-$ NPCs. Because CD140a-depleted cells do not readily undergo oligodendrocyte differentiation, but likely represent their immediate developmental precursor, we induced the expression of potentially instructive OPC TFs in human NPCs by lentiviral overexpression. We found that although several TFs were capable of driving the expression of OPC-specific enhancer elements and individual genes, only SOX10 induced genome-wide reprogramming to resemble human CD140a-defined OPCs. Furthermore, enforced SOX10 expression alone was sufficient to induce oligodendrocyte differentiation at equivalent levels to native OPCs in vitro and to enhance the rate of differentiation and myelination of xenografted NPCs in hypomyelinating *shiverer/rag2* mice.

Results

FACS-Array Identification of Human OPC-Induced and Specific TFs. To select TFs in an unbiased manner, we performed microarray analysis on FACS-isolated human progenitor populations. We directly compared CD133$^+$CD140a$^-$ neural progenitor cells with

Significance

Transplantation of human myelinogenic cells represents a realizable strategy for treatment of congenital and acquired demyelinating diseases. Although generation of undifferentiated neural stem and progenitors is feasible, the induction of myelinogenic cell fate remains a significant challenge. In this paper, we describe, to our knowledge, the first comprehensive study of transcription factor expression and function by purified neural and oligodendrocyte progenitors obtained directly from human brain tissue. We have identified those transcription factors capable of regulating oligodendrocyte progenitor fate and establish that among these, only SOX10 was capable of comprehensively inducing oligodendrocyte fate both in vitro and following transplantation into a model of human leukodystrophy. Thus, viral and pharmacologic approaches to increasing SOX10 expression likely will improve the outcome of human transplant therapy.

Author contributions: J.W. and F.J.S. designed research; J.W., S.U.P., A.K.H., C.W., M.A.O., and F.J.S. performed research; J.W. and F.J.S. analyzed data; and J.W. and F.J.S. wrote the paper.

The authors declare no conflict of interest.

This article is a PNAS Direct Submission.

[1]To whom correspondence should be addressed. E-mail: fjsim@buffalo.edu.

This article contains supporting information online at www.pnas.org/lookup/suppl/doi:10.1073/pnas.1408295111/-/DCSupplemental.

committed OPCs defined by $CD133^+CD140a^+$ antigenicity (15) as well as with CD140a/O4-defined OPCs. We identified 12 TFs that were up-regulated during the specification of OPC fate and/or between $O4^+$ oligodendrocyte-biased and bipotential CD140a/$PDGF\alpha R^+$ OPCs (Fig. S1). We confirmed the expression profiles of these TFs using quantitative RT-PCR (qPCR) (Fig. S2), and selected a subset of eight TFs for further functional analysis. We also chose ASCL1 because it has been shown to be necessary and sufficient to induce immature oligodendrocyte fate from mouse neural progenitors (17).

A Subset of OPC TFs Activate the *Sox10*-MCS5 Enhancer in Human NPCs. We selected a species conserved SOX10 enhancer as an initial screen of OPC fate induction. We recently found that the *Sox10*-MCS5 enhancer is differentially active in human CD140a-defined OPCs compared with native $CD133^+CD140a^-$ NPCs (15), and can be used to identify human OPCs (18). At 24 h after isolation, NPCs were infected with a *Sox10*-MCS5:GFP reporter virus and a candidate TF or mCherry-expressing virus as a negative control. Matched $CD140a^+$ OPCs were used as a positive control in this and all other experiments. GFP expression was first detected in $CD140a^+$ cells after 2 d and increased in intensity thereafter. Mean GFP intensity was measured at 3–4 d by flow cytometry (n = 3–9 fetal samples) (Fig. 1). As expected, $CD140a^+$ OPCs expressed high levels of GFP, >2.8 fold greater than that expressed by uninduced NPCs ($P < 0.05$).

We found that ASCL1, NKX2.2, and SOX10 were each capable of significantly inducing *Sox10*-MCS5 enhancer activity ($P < 0.01$, normalized to mCherry control). None of the other factors induced GFP expression. Apart from ASCL1, all other factors drove enhancer activity at significantly lower levels than $CD140a^+$ OPCs ($P < 0.05$, Dunnett's post hoc test). These data indicate that ASCL1, NKX2-2, SOX10, and, to a lesser extent, OLIG2 and SOX8, regulate *Sox10* enhancer activity in human NPCs.

Single TF Infection Can Induce Markers of OPC Fate. We next asked whether enforced TF expression could lead to induction of OPC markers. Following infection, NPCs were maintained for 4–7 d before RNA extraction or immunocytochemistry (Fig. 2). For qPCR, we selected PDGFRA and CSPG4, encoding $PDGF\alpha R$/CD140a and NG2 proteins, respectively. As expected, PDGFRA mRNA was highly enriched in $CD140a^+$ OPCs, by 13.5-fold relative to mCherry-infected NPCs, whereas CSPG4 mRNA enrichment was 3.2-fold higher (n = 3–5 fetal preparations) (Fig. 2*A*). Several of the candidate TFs induced CSPG4 mRNA, including ASCL1, NKX2.2, and SOX10 ($P < 0.05$, Dunnett's post hoc test, repeated-measures one-way ANOVA). Interestingly, ASCL1 induced significantly higher expression of CSPG4 mRNA than native OPCs ($P < 0.05$, paired t test). In contrast, only ASCL1 was able to up-regulate PDGFRA mRNA (Fig. 2*B*). Several factors, including NKX2.2 and PRRX1, seemingly repressed PDGFRA expression. To control for the effect of media on induction of these markers, we performed parallel experiments in both PDGF/FGF- and EGF/FGF- containing media (n = 2 fetal preparations), and found that gene expression changes were similar regardless of growth conditions.

We examined expression of antigenic markers of OPC fate using NG2- and A2B5-specific antibodies (Fig. 2 *C*–*L*). NPCs were infected and maintained in culture for 7 d in PDGF-AA/FGF supplemented media. $CD140a^+$ OPCs maintained in the same medium conditions were found to express high levels of both A2B5 and NG2. In control mCherry-infected NPCs, only 2.6 ± 0.5% expressed A2B5 (n = 3 fetal samples). In contrast, OLIG2, PPRX1, and SOX10 overexpression significantly induced A2B5 in 23–64% of NPCs ($P < 0.05$, Dunnett's post hoc test, one-way ANOVA). Unlike A2B5, NG2 expression was not induced following OLIG2 overexpression, but was significantly induced in SOX10-, NKX2.2-, and PRRX1-infected cells. SOX10 consistently induced >60% of the infected NPCs to express both NG2 and A2B5.

Interestingly, the morphology of SOX10-infected $NG2^+$ cells was altered such that several exhibited a flatter multipolar morphology compared with the bipolar appearance of native $CD140a^+$ OPCs. ASCL1-infected NPCs rapidly underwent changes in cell morphology, becoming more fusiform and often with an enlarged bipolar appearance. We examined the expression of NG2 and A2B5 at 4 d and found that ASCL1 overexpression increased the abundance of both markers relative to mCherry-infected cells (Fig. 2 *K* and *L*). Taken together, these data indicate that ASCL1 and SOX10 have a strong effect on Sox10 enhancer, OPC marker mRNA, and protein expression; NKX2.2, OLIG2, and PRRX1 have a weaker effect on a subset of these markers; and only ASCL1 is capable of inducing PDGFRA mRNA.

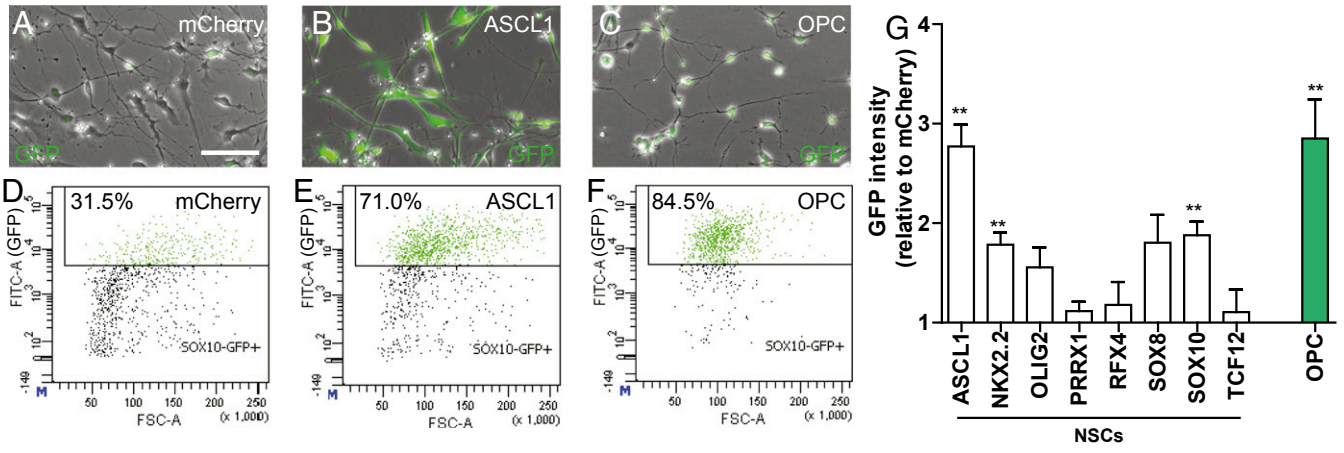

Fig. 1. OPC-specific TFs selectively activate Sox10-MCS5 enhancer. Human $CD133^+CD140a^-$ NPCs were coinfected with Sox10-MCS5:GFP reporter virus and individual OPC-specific TFs or mCherry control virus following isolation. (*A*–*C*) In contrast to control NPCs (mCherry), ASCL1-infected NPCs and OPCs contained a high proportion of cells expressing GFP at high levels (4 d in vitro). (*D*–*F*) Flow cytometry analysis of GFP expression, GFP^{high}% (1,000 events shown). (*G*) Quantification of mean GFP intensity relative to matched mCherry control (mean ± SEM; n = 4–9 fetal samples). **Indicates a significant increase in GFP expression; $P < 0.01$. (Scale bar: 100 μm.)

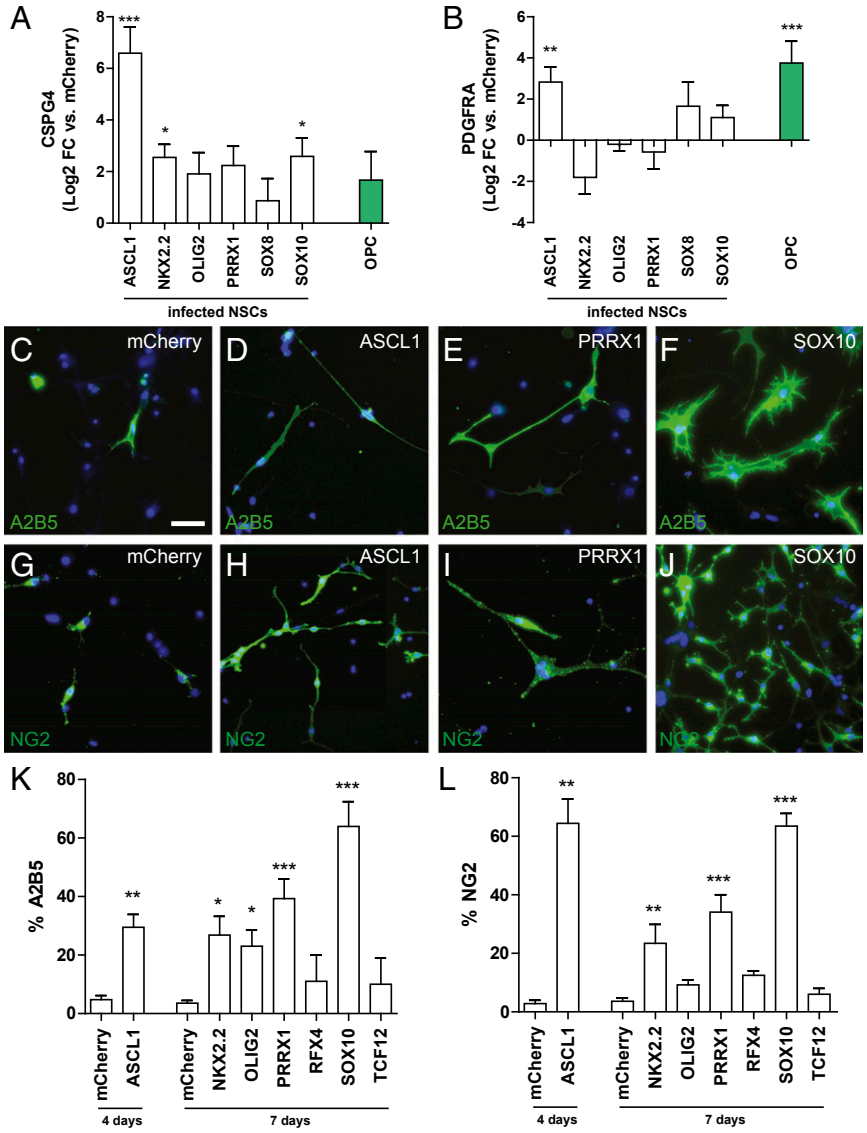

Fig. 2. Induction of OPC-specific genes by individual factors. Sorted CD133$^+$CD140a$^-$ NPCs infected with lentivirus were analyzed at 7 d by qPCR and immunocytochemistry. (*A* and *B*) qPCR analysis of OPC-specific genes *CSPG4* and *PDGFRA* (n = 3–5 fetal brain preparations). Gene expression of TF-infected NPCs and uninfected OPCs is shown relative to mCherry-infected controls (log-twofold change, mean ± SEM; GAPDH-normalized). * $P < 0.05$; ** $P < 0.01$; *** $P <$ 0.001, Dunnett's posttest (one-way ANOVA). (*C–J*) Infected NPCs were immunostained with OPC markers A2B5 (*C–F*) and NG2 (*G–J*) and nuclei counterstained with DAPI (blue). Matching cultures were fixed at 4 d and 7 d. (*K* and *L*) Quantification of A2B5% (*K*) and NG2% (*L*) (mean ± SEM, n = 3–5). * $P < 0.05$; ** $P <$ 0.01. (Scale bar: 50 μm.)

SOX10 Expression Induces an OPC-Like Gene Expression Signature. We next sought to determine whether TF overexpression would regulate OPC-specific gene expression on a genome-wide scale. We performed Illumina microarray analysis for ASCL1-, SOX10-, and NKX2.2-infected NPCs and compared their expression with that in matched mCherry controls (n = 2 fetal preparations). We noted that the expression profiles of both ASCL1- and NKX2.2-infected cells were distinct from the profiles of mCherry-infected cells and also of each other, indicating divergent effects on gene expression (Fig. 3*A*).

Because the microarray probes for ASCL1, SOX10, and NKX2.2 are not located within the coding region of each gene, we examined the endogenous regulation of each factor (Fig. 3*B*). As such, ASCL1 might induce its own expression while repressing NKX2.2 expression. SOX10 overexpression did not regulate these TFs. All three TFs reduced astrocyte-specific gene expression, including intermediate filament GFAP and glutamate transporter GLT-1 (SLC1A2). Neuronal-expressed transcripts, such as CD24 and doublecortin (DCX), were up-regulated after ASCL1 overexpression (by 9.6- and 15.9-fold, respectively). NKX2.2 similarly up-regulated CD24 (by 3.7-fold) and neuronal RNA-binding protein HuD (ELAVL4, by 7.3-fold). In contrast, SOX10 did not regulate neuronal markers. Both SOX10 and ASCL1 induced OPC-specific transcripts NG2 (CSPG4) and PDGFRA. SOX10 also induced the A2B5 synthetic enzyme ST8SIA1, as well as myelin transcripts PLP1 and UGT8 (Fig. 3*C*). Each TF also was capable of regulating a subset of specific OPC-expressed TFs, suggesting a hierarchy of TF activation in human NPCs (Fig. 3*D*).

Among ASCL1-induced genes, we found a very significant overrepresentation of genes involved in cell cycle and proliferation (topGO enrichment analysis, $P = 1.2 \times 10^{-25}$). In contrast, NKX2.2 up-regulated genes involved in regulation of synaptogenesis

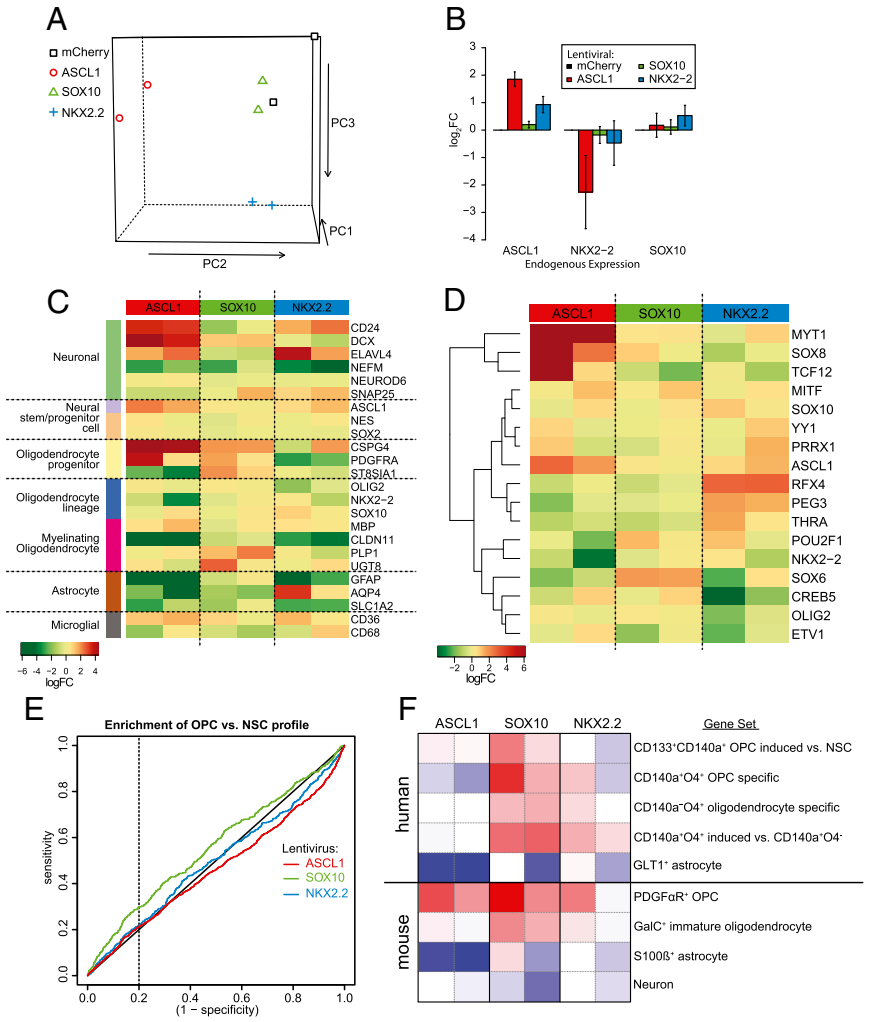

Fig. 3. SOX10 induces an OPC-like profile of gene expression. To determine the effect of each TF on NPC transcriptional profiles, RNA was extracted from infected cells at 7 d and profiled using microarray. (*A*) Principal component analysis of all expressed genes revealed large differences in gene expressed following TF overexpression. (*B*) The effect of TF on endogenous expression was determined using probes binding 3′ UTR sequences. Bar chart shows log-fold change following normalization to mCherry (mean ± SEM, $n = 2$). (*C*) Heatmap showing gene expression of cell-type restricted genes for each sample following infection. Scale indicates expression relative to matched mCherry profile. (*D*) Regulation of OPC-specific TFs following virus infection relative to mCherry. (*E* and *F*) ROC and gene set enrichment analysis (GSEA) after TF overexpression. (*E*) ROC analysis of virally induced genes versus the profile of $CD133^+$ $CD140a^+$ OPCs relative to $CD133^+CD140a^-$ NPCs. The deflection of each line above the 'line of identity' (black diagonal) indicates enrichment of genes induced compared with mCherry infection. (*F*) GSEA examining relative enrichment of cell-type specific genes among virally induced gene signatures. Red indicates enrichment; blue, depletion.

($P = 2.9 \times 10^{-3}$) and down-regulated genes involved in the PDGFR signaling ($P = 2.5 \times 10^{-3}$).

To determine whether TF overexpression induced OPC-specific gene expression, we directly compared the enrichment of TF-induced genes among the profile of human $CD133^+CD140a^+$ OPCs with that of the $CD133^+CD140a^-$ NPCs from which they are derived (Fig. 3*E*). We found that only SOX10-induced genes were enriched among native OPCs relative to NPCs, and that this enrichment was highly significant ($P = 2.1 \times 10^{-4}$).

We next used gene set enrichment analysis to include multiple gene expression signatures specific to sorted human and mouse cells (14, 19) (Fig. 3*F*). ASCL1 significantly regulated mouse OPC genes but did not induce a human OPC gene expression signature, suggesting that ASCL1 overexpression might be differentially capable of inducing OPC fate in mouse NPCs, but not in human NPCs. In contrast, we found that SOX10 overexpression significantly induced genes expressed by both human and mouse OPCs while repressing neuronal and astrocyte genes (false discovery rate-adjusted q value <.05). Importantly, SOX10-induced genes also associated with oligodendrocyte commitment in both species (human $CD140a^-O4^+$ and mouse GalC profiles), suggesting that SOX10 overexpression would permit both OPC and oligodendrocyte fate commitment.

SOX10-Induced OPCs Are Capable of Oligodendrocyte Commitment in Vitro. One hallmark of OPCs is their ability to expand in the presence of mitogens and undergo oligodendrocyte differentiation following mitogen withdrawal. To determine whether infected cells could differentiate as oligodendrocytes, we allowed infected NPCs serially grown in the presence of FGF-2/EGF (4 d) then FGF/PDGF-AA (6 d) to differentiate in the absence of mitogens at day 10 before fixation at 14 or 21 d (Fig. 4). On day 14, 21.6 ± 2.9% uninfected CD140a-sorted OPCs differentiated into $O4^+$ immature oligodendrocytes with typical branched morphology ($n = 3$–8 fetal preparations), and some matured into myelin sheet-forming oligodendrocytes (Fig. 4*D*, arrowhead). In comparison, few mCherry-infected control NPCs were $O4^+$ (0.2 ± 0.2%). Likewise, individual overexpression of ASCL1, NKX2-2, OLIG2, and PRRX1 did not induce oligodendrocyte fate (Fig. 4). However, SOX10 infection induced a significant amount of immature oligodendrocytes (16.8 ± 3.2%), surprisingly close to the uninfected OPCs. Most SOX10-induced oligodendrocytes had the same morphology as those derived from primary OPCs (Fig. 4*C*).

Although not a specific marker of OPCs (20), OLIG2 is required for normal oligodendrocyte lineage differentiation (21) and is expressed by all oligodendrocyte lineage cells. As such, we colabeled cultures with OLIG2 to determine whether TF overexpression regulated OLIG2 expression (Fig. 4 *A*–*D* and *F*). Similar to acutely isolated $CD133^+CD140a^-$ NPCs (15), ∼30% of mCherry-infected NPCs expressed OLIG2 protein. As expected, OLIG2 virus induced very strong OLIG2 protein expression (83 ± 9%; $n = 3$ fetal preparations). None of the other TFs up-regulated OLIG2. Interestingly, all SOX10-induced $O4^+$ oligodendrocytes coexpressed OLIG2, suggesting that endogenous OLIG2 is

required for oligodendrocyte reprogramming. In contrast, ASCL1 overexpression induced a greater than fivefold increase in Tuj1$^+$ neuron generation, along with concomitant near abolition of OLIG2 expression (1.3 ± 0.7%, $n = 3$; $P < 0.05$, one-way ANOVA) (Fig. 4*F*). Interestingly, combined ASCL1 and OLIG2 overexpression also gave rise to neuronal induction.

Because OPC-expressed TFs may act to inhibit premature terminal differentiation, we asked whether transient overexpression

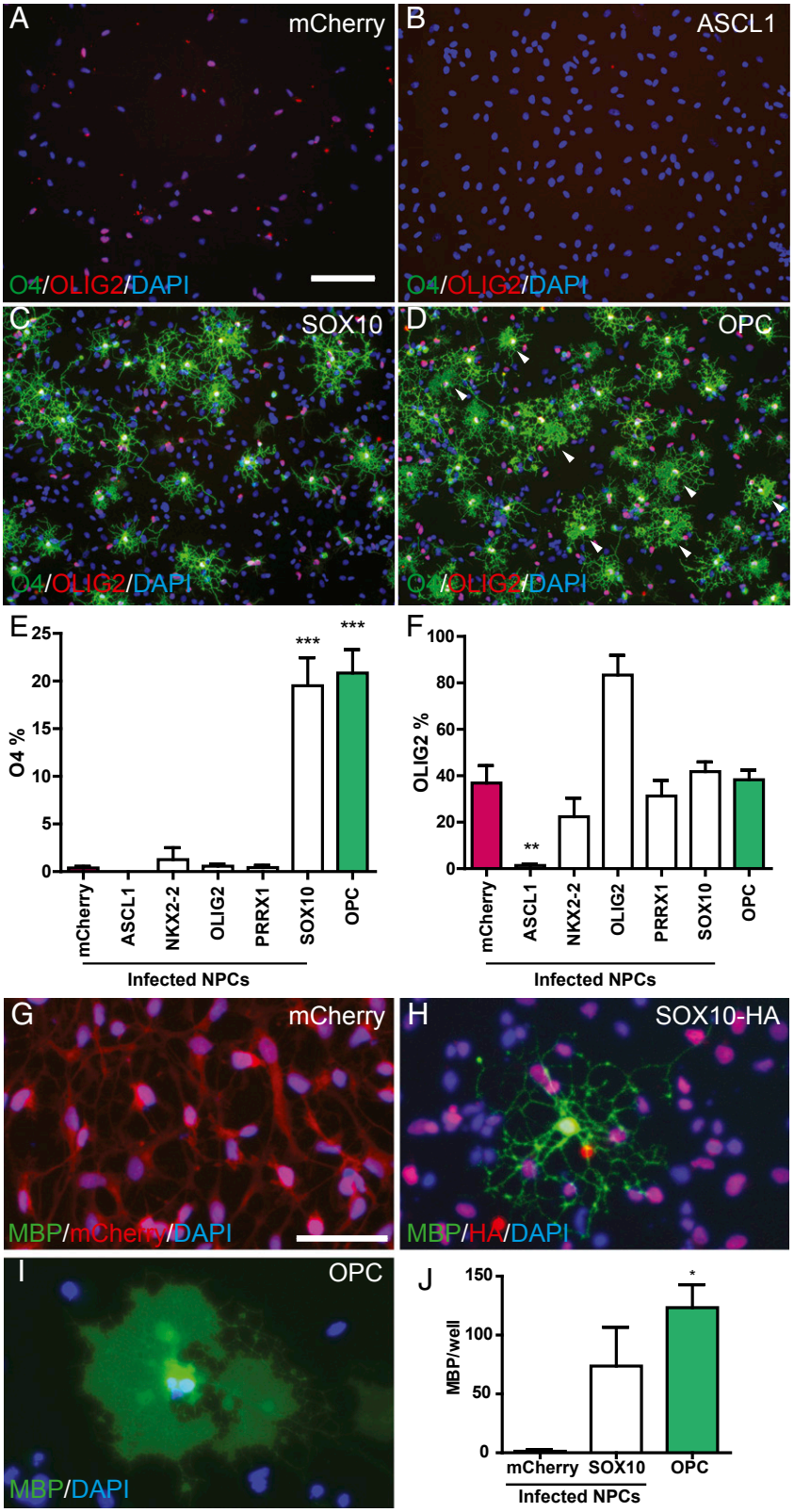

Fig. 4. SOX10-induced NPCs undergo oligodendrocyte commitment in vitro. Uninfected OPCs, NPCs infected with either mCherry control virus or individual TF were maintained in pro-oligodendrocyte conditions for 14–21 d. (*A–D*) Cultures were immunostained with OLIG2 (red) and immature oligodendrocyte marker O4 (green) at day 14. (*E* and *F*) Quantification of OLIG2% and O4% (mean ± SEM; $n = 3$–6 fetal preparations). (*G–I*) Cultures maintained for up to 21 d were MBP immunostained to label mature oligodendrocytes. MCherry- and SOX10-HA–infected cells were visualized using mCherry fluorescence and anti-HA antibody, respectively. (*J*) Quantification of MBP$^+$ cells per well (mean ± SEM; $n = 3$ fetal preparations). *$P < 0.05$; **$P < 0.01$; ***$P < 0.001$ vs. mCherry control (one-way ANOVA, Dunnett's posttest). (Scale bars: 100 μm in *A–D*; 50 μm in *G–I*.)

may permit oligodendrocyte differentiation following mitogen withdrawal. Using a doxycycline-inducible lentiviral vector, we overexpressed candidate TFs, ASCL1, PRRX1, and SOX10 for 2 or 4 d in human NPCs. As with constitutive overexpression, transient overexpression was sufficient to induce NG2 expression at 7 d (Fig. S3); however, after mitogen removal, only SOX10 was capable of inducing $O4^+$ oligodendrocytes. This finding suggests that the absence of oligodendrocyte differentiation following PRRX1 and ASCL1 is not limited by direct inhibition of differentiation.

To determine whether SOX10-infected NPCs are capable of maturation to MBP^+ oligodendrocytes, we fixed matched cultures at 21 d (Fig. 4 *G–J*). As expected, primary $CD140a^+$ OPCs generated numerous oligodendrocytes with MBP^+ myelin sheets (123 ± 19 cells/well, $n = 3$ fetal dissociates), whereas very few oligodendrocytes were observed in cultures of mCherry-infected NPCs (1.3 ± 1.3 cells/well). SOX10-infected NPCs generated a substantial number of MBP^+ oligodendrocytes with a highly branched complex morphology. Using a HA-tagged SOX10 virus, we found that all MBP^+ cells retained SOX10-HA expression at 21 d. Of the OPC-expressed TFs tested, only SOX10 was sufficient to induce rapid oligodendrocyte differentiation from primary human NPCs in vitro.

SOX10-Infected NPCs Are Proliferative Oligodendrocyte Progenitors in Vitro. Primary human OPCs differentiate in a context-specific manner and can be maintained as progenitors for several passages in vitro (22). To determine whether SOX10-infected NPCs could be maintained as proliferative progenitors, we grew mCherry- and SOX10-HA–tagged NPCs in the presence of PDGF-AA for three passages (>1 mo in vitro) and assessed oligodendrocyte differentiation at each passage (Fig. S4). No between-group differences in cell expansion were noted. A 24-h BrdU pulse before fixation revealed that the majority of SOX10-HA–expressing cells were proliferative while maintained in PDGF-AA and FGF-2. In addition, $SOX10\text{-}HA^+$ cells colabeled with NG2 expression, whereas matched mCherry-infected cultures exhibited few $NG2^+$ cells. Significantly, spontaneous differentiation of $O4^+$ oligodendrocytes was not observed in cultures maintained in growth factors.

In an experiment to test whether SOX10-infected NPCs could still differentiate, infected cells were pulsed for 24 h with BrdU and then grown in the absence of mitogens for 4 d and stained. At each passage, several SOX10-HA–infected cells differentiated as $O4^+$ oligodendrocytes. Importantly, even at the third passage, we observed $SOX10\text{-}HA^+O4^+BrdU^+$ cells, indicating that recently dividing SOX10-infected cells were able to undergo differentiation after mitogen withdrawal (Fig. S4). Taken together, these data suggest that SOX10 overexpression induces a proliferative progenitor that retains the capacity for oligodendrocyte differentiation similar to that of native OPCs.

SOX10 Overexpression Induces Rapid Myelination from Human NPCs. To determine the myelinogenic capacity of SOX10-infected NPCs, we injected 1×10^5 infected human NPCs into the corpus callosum of neonatal *shiverer/rag2* mutant mice. NPCs were infected with either SOX10- or mCherry-expressing virus at 48 h before implantation. At 12 wk postimplantation, both mCherry- and SOX10-infected human NPCs exhibited a similar pattern of engraftment. Human cells (hNA^+) were observed from olfactory bulbs to the caudal extent of fimbria, spanning >5 mm in all transplanted mice. Typically, transplanted human cells were located in white matter, such as corpus callosum, fimbria, and striatal white matter. Overall human cell engraftment was greater in callosum (550 ± 43 hNA^+ cells/mm^2) than in fimbria (140 ± 7 hNA^+ cells/mm^2).

We first assessed the effect of SOX10 overexpression on oligodendrocyte differentiation and maturation. At 12 wk posttransplantation, SOX10-infected NPCs underwent robust differentiation as CC1- and MBP-expressing oligodendrocytes. Importantly, SOX10 overexpression resulted in an almost twofold increase in the proportion of human hNA^+ cells undergoing differentiation as hNA^+CC1^+ oligodendrocytes in the corpus callosum (mean ± SEM, 27 ± 4% vs. 14 ± 2%; $P < 0.05$, unpaired t test; $n = 3$) (Fig. 5 *A* and *B*). Although myelin basic protein (MBP) expression was produced by both engrafted groups (Fig. 5*C*), in the fimbria where individual MBP^+ oligodendrocytes could be reliably counted, we found significantly more MBP^+ oligodendrocytes derived from SOX10-infected NPCs compared with matched mCherry-infected cells (25 ± 2% vs. 14 ± 1%; $n = 3$ animals per group) (Fig. 5 *D*, *E*, and *K*).

In addition, we noted a profound difference in the intracellular distribution of MBP between mCherry and SOX10-infected cells in the corpus callosum (Fig. 5 *F* and *G* and Fig. S5). MBP was localized in the cell body of human oligodendrocytes derived from mCherry-infected NPCs, whereas MBP was exclusively localized to axonal segments in animals receiving SOX10-infected NPCs. Because differential localization of MBP has been associated with progressive myelination by human cells (3), we compared the efficiency of callosal axonal ensheathment by each cell type (5) (Fig. 5 *H–J*). SOX10-infected NPCs ensheathed >30% of axons in the corpus callosum (32 ± 1%; $n = 3$ animals), more than twice the proportion ensheathed by mCherry-infected cells. Importantly, the extent of ensheathment by SOX10-infected NPCs exceeded that of human iPSC-derived glial progenitors at 13 wk (10), and was equivalent to that of native fetal CD140a-defined OPCs at this time point (5). Taken together, these data indicate that oligodendrocyte differentiation and myelinogenesis from primary NPCs is induced by enforced SOX10 expression, and that SOX10-induced neural stem cells produce myelin at a similar rate as native human OPCs.

SOX10-Infected NPCs Resemble Native OPCs after Engraftment in *Shiverer* Mice. Given that SOX10 overexpression significantly increased oligodendrocyte differentiation and myelination by human NPCs in vivo, we asked whether this effect is related to regulation of NPC homeostasis, increased OPC specification, and/or differentiation. Human nestin-positive NPC-expressing cells were found in the corpus callosum in both groups of animals at 12 wk (Fig. 6*A*). Several nestin-positive cells were located surrounding the lateral ventricles and extended processes through the ependymal layer and as such morphologically resembled native neural stem cells (Fig. 6*A*, *Inset*). Thus, transplanted NPCs persisted in the murine parenchyma after transplantation.

Importantly, we found no quantitative between-group difference in cell density ($n = 3$ per group, unpaired t test). The proportion of mCherry and SOX10-infected cells expressing markers of proliferation was also similar in the two groups. Among scored animals, the fraction of $Ki67^+hNA^+$ cells was 9.5 ± 0.6%, similar to that of primary $CD140a^+$ OPCs (5). More importantly, SOX10-HA–expressing cells were still proliferative at 12 wk, expressing Ki67 and PCNA (Fig. 6*B*). These data suggest that SOX10 overexpression does not induce differentiation at the cost of reduced cell engraftment, migration, and proliferation.

At 8 wk posttransplantation, significant numbers of human $NG2^+$ OPCs were found in the corpus callosum and fimbria of animals receiving SOX10-induced OPCs (Fig. S6). In contrast, few mCherry-infected NPCs expressed NG2. By 12 wk, human $NG2^+$ cells pervaded the corpus callosum and forebrain white matter in both groups, and no obvious differences in OPC density were observed (Fig. 6*C*). Examination of oligodendrocyte differentiation at 8 wk showed that significantly more SOX10-infected NPCs differentiated as $CC1^+hNA^+$-differentiated human oligodendrocytes compared with mCherry control ($P < 0.05$, t test) (Fig. S6 *E–G*). Furthermore, although very few MBP^+

mature oligodendrocytes were observed in mCherry-infected NPC-engrafted animals at 8 wk, MBP$^+$ cells were diffusely present throughout the corpus callosum and fimbria of all SOX10-transplanted mice (n = 3 per group) (Fig. S6 *H–K*). These data suggest that SOX10-infected NPCs resemble native OPCs in several respects, retaining mitotic competence and NG2$^+$ expression for several months and progressively differentiating as MBP$^+$ oligodendrocytes in vivo.

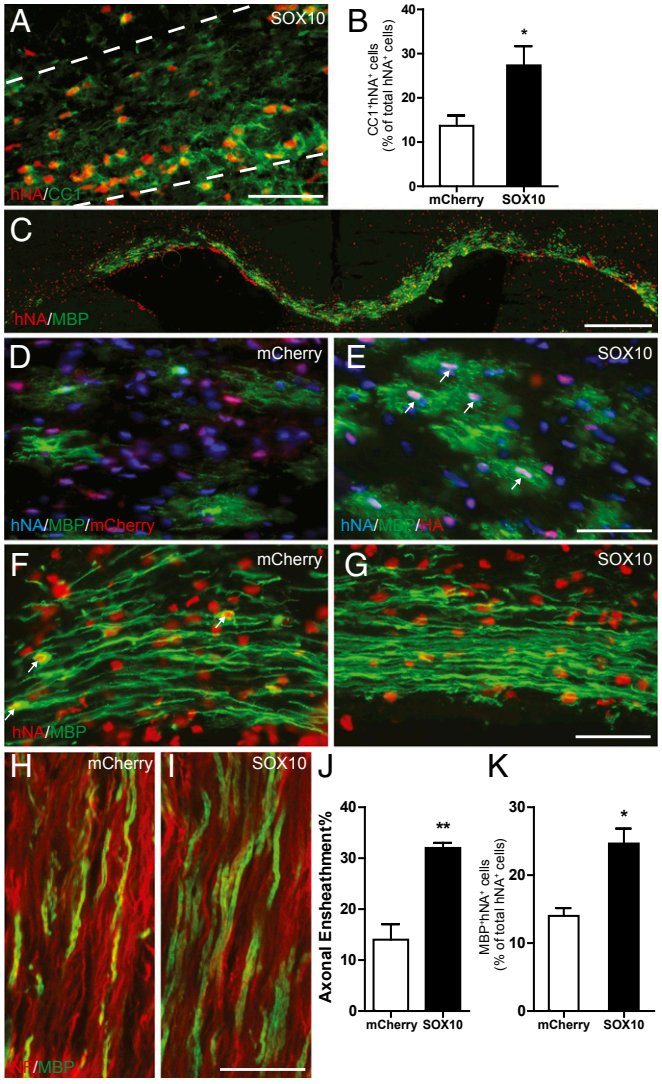

Fig. 5. SOX10-infected NPCs rapidly myelinate the *shiverer/rag2* brain. Human NPCs infected with either mCherry or SOX10 lentivirus were injected into neonatal *shiverer/rag2* mice and examined at 12 wk. (*A*) Human cells were identified using human nuclear antigen (hNA, red) and oligodendrocytes using CC1 (green). (*B*) The proportion of human cells undergoing CC1$^+$ oligodendrocyte differentiation was counted in the corpus callosum (mean ± SEM; n = 3 animals per group). (*C*) Donor-derived myelination defined by MBP-staining (green) was apparent throughout the corpus callosum in animals receiving either mCherry- or SOX10-infected NPCs. (*D* and *E*) Individual MBP$^+$ (green) oligodendrocytes could be identified in the fimbria, and the proportion of oligodendrocytes was counted (*K*). Viral expression was maintained at 12 wk as defined by mCherry (red) or HA-tagged SOX10 (red) protein labeling. (*F* and *G*) In the corpus callosum, the intracellular pattern of MBP expression differed significantly between groups. In contrast to mCherry-infected NPCs, SOX10-infected NPCs exhibited dense parallel alignment of the MBP process and did not exhibit cell body-localized MBP ensheathment of host mouse axons (neurofilament, red) at 12 wk by mCherry-infected (*F*) or SOX10-infected (*G*) NPCs. (*H* and *I*) Ensheathment efficiency of mCherry-infected (*H*) and SOX10-infected (*I*) NPCs was quantified in the corpus callosum (mean ± SEM; n = 3). (*J*) quantification of donor-derived MBP$^+$ oligodendrocytes in fimbria; see *D* and *E* (mean ± SEM; n = 3). (Scale bars: 50 μm in *A* and *D–G*; 200 μm in *C*; 20 μm in *H* and *I*.) *P < 0.05; **P < 0.01 vs. mCherry control, unpaired t test.

SOX10 Overexpression Inhibits Astrocytic Commitment from NPCs. Because human CD140a$^+$ OPCs also differentiate into fibrous astrocytes following transplantation (5), we determined the proportion of infected human NPCs that expressed GFAP$^+$ astrocytes at 12 wk (Fig. 6 *D–F*). Interestingly, SOX10 overexpression significantly impaired the production of GFAP$^+$ astrocytes compared with mCherry-infected NPCs (quantified in the corpus callosum; 18 ± 3% in SOX10-infected vs. 40 ± 5% in mCherry-infected; unpaired t test, n = 3) (Fig. 6*F*). We hypothesized that the quantitative level of SOX10 expression in OPCs could influence oligodendrocyte differentiation. To directly test this hypothesis, we infected primary human CD140a$^+$ OPCs with SOX10 or mCherry lentivirus and assessed oligodendrocyte and astrocyte differentiation at 4 d after infection (Fig. S7). Consistent with our in vivo data, enforced SOX10 expression induced O4$^+$ oligodendrocyte differentiation at the cost of GFAP$^+$ astrocytic commitment. Taken together, these data indicate that SOX10 overexpression is not only capable of inducing rapid OPC fate commitment, but also promotes myelinogenic oligodendrocyte differentiation from human NPCs.

Discussion

Identification of OPC-Specific TFs. In this study, we sought to identify TFs that may regulate human OPC fate during fetal development. We hypothesized that TF up-regulation of inductive factors would coincide with acquisition of OPC fate. We chose CD140a/PDGFaR antigen because it represents an early and specific marker of human OPCs (5). Through a combination with CD133, we were able to distinguish CD133$^+$CD140a$^-$ NPCs from CD140a$^+$ OPCs (15). Genomic analysis of CD140a$^+$ OPCs relative to NPCs identified known OPC-specific TFs, including SOX10, OLIG2, NKX2.2, MYT1, ID2, and HES5 (23). In contrast, our analysis did not identify TFs that specifically regulate oligodendrocyte differentiation (e.g., MYRF, ZNF488, NKX6.2). This approach allowed us to identify TFs expressed by OPCs at the time of specification. It is conceivable, however, that key TFs may be transiently up-regulated during transition to OPC fate, and that isolation of OPCs en masse would not be resolved.

In addition to known TFs, we identified several previously unidentified OPC-expressed TFs. In addition to fetal OPCs, PRRX1, a paired-type homeodomain factor, is also highly expressed in human adult OPCs (14) and rodent OPCs (19, 24). We found that PRRX1 overexpression induced OPC antigens A2B5 and NG2, suggesting that it may directly induce OPC fate; however, by itself, it was not sufficient to permit oligodendrocyte differentiation. Interestingly, ectopic PRRX1 is known to inhibit neuronal differentiation of adult murine NPCs and thereby promote self-renewal (25). RFX4, a winged helix DNA-binding protein, is up-regulated in fetal OPCs compared with NPCs, and its expression is maintained in adult human OPCs (14). Interestingly, RFX4 is highly expressed by both human and mouse astrocytes as well, suggesting a role in both glial subtypes (14, 19). Knockout of RFX4 down-regulates Wnt ligand and induces Id4 expression in early embryonic brain, implicating it in the specification and development of glia (26); however, RFX4 overexpression does not affect expression of OPC markers in human NPCs, and a precise role in glia remains to be determined. Both POU2F1 (Oct-1) and TCF12 likely act as accessory transcriptional regulators to SOX and class B bHLH proteins, respectively. Although widely expressed in development, the quantitative increase in POU2F1 and TCF12 mRNAs

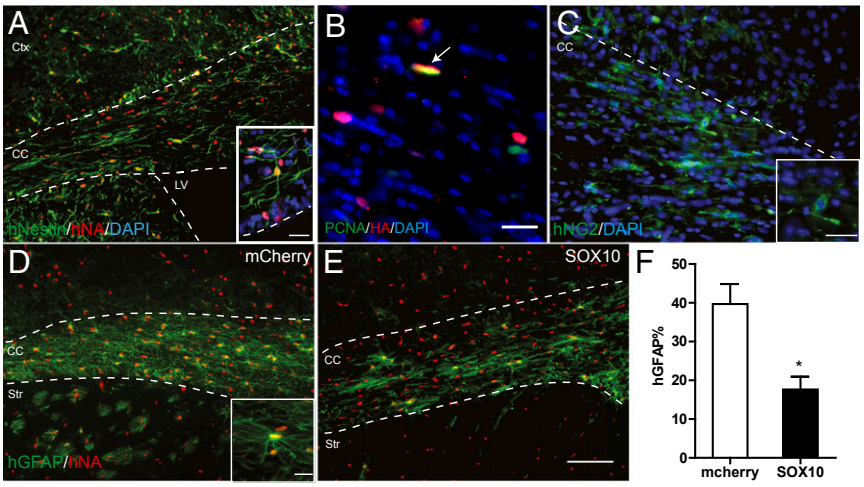

Fig. 6. SOX10 overexpression inhibits astrocytic commitment from NPCs. The neural lineage commitment of transplanted NPCs was assessed at 12 wk using human-specific antibodies to detect donor cells. (*A*) Transplanted cells expressing nestin were identified using hNestin (green) and hNA (red). Nestin-positive NPCs were found throughout the engrafted region including the corpus callosum (CC), striatum, and inner layers of the cortex (Ctx). Human nestin-positive cells were often found to extend processes into the lateral ventricle (*A*, *Inset* and *B*) A small fraction of transplanted SOX10-HA$^+$ human cells remained mitotically active at 12 wk, labeled with PCNA (green) and HA (red). (*C*) Human OPCs were stained with human-specific NG2 antibody (hNG2, green) in the corpus callosum; insert, a single NG2$^+$ OPC. (*D* and *E*) Donor-derived astrocytes were visualized using human-specific GFAP antibody (green) and hNA (red). Significantly more hGFAP$^+$ astrocytes were derived from mCherry-infected NPCs than from SOX10-infected cells. (*F*) The proportion of hGFAP$^+$ astrocytes among hNA$^+$ donor cells was counted in the corpus callosum (mean ± SEM; $n = 3$). *$P < 0.05$ vs. mCherry control, *t* test. (Scale bars: 100 μm in *A*, *B*, *D*, and *E*; 20 μm in *C* and *Insets*.)

in CD140a$^+$ OPCs suggests a role in OPC specification that was not revealed by overexpression.

Induction of Human OPC and Oligodendrocyte Fate. Because NPCs represent the direct developmental forbears of OPCs, we hypothesized that overexpression of a single TF would direct OPC and oligodendrocyte fate. By defining the TF factor/s sufficient to induce fate, we anticipated that success would permit mechanistic analysis of TF activity in NPCs before the analysis of TF combinations. The induction of oligodendrocyte fate by individual TF overexpression has been studied in several model organisms, including zebrafish, chick, and mouse. It appears that multiple TFs can induce oligodendrocyte differentiation from neural precursors, including OLIG1/2, NKX2.2, ASCL1, SOX10, SOX17, and others (17, 27–34); however, the instructive role of individual factors toward oligodendrocyte fate has not been observed consistently across species and systems. For example, ASCL1 is capable of inducing rapid oligodendrocyte differentiation in cultured mouse neural stem/progenitors (17), but retroviral-mediated expression in embryonic mouse forebrain does not induce oligodendrocyte fate (32). In human fetal neurospheres, OLIG2 overexpression leads to increased expression of A2B5 that does not yield significant oligodendrocyte differentiation in *shiverer* mice (35). As such, the robust induction of OPC and oligodendrocyte fate from human NPCs by TF overexpression has not yet been achieved.

Because expression of individual markers such as A2B5, NG2, and OLIG2 is not restricted to OPCs, we sought to define OPC fate through a combination of marker expression, activity of known enhancer elements, genome-wide expression profiles, and functional characteristics, growth factor proliferation and oligodendrocyte differentiation. These results are summarized in Table S1. Of the factors tested, only SOX10 overexpression was capable of inducing a proliferative progenitor cell that rapidly differentiates into oligodendrocytes both in vitro and in vivo.

Context-Specific Effects of TF Overexpression. When induced to differentiate by mitogen withdrawal, SOX10-infected NPCs generated equivalent numbers of O4$^+$ and MBP$^+$ oligodendrocytes to native primary CD140a-sorted OPCs. Induced oligodendrocytes were restricted to the OLIG2-expression fraction of NPCs. This suggests that OLIG2 is necessary for OPC fate, as has been demonstrated in rodents (31, 36). Interestingly, coinfection with SOX10 and OLIG2 viruses did not result in a significant increase in O4$^+$ oligodendrocyte differentiation, suggesting that OLIG2 is not the sole limiting factor for OPC fate induction by SOX10. Indeed, because both binding partners (37) and phosphorylation state (38) can regulate the function of OLIG2, overexpression of OLIG2 alone might not provide the correct cellular context for induction of OPC fate.

Likewise, we observed that whereas ASCL1 or PRRX1 overexpression was sufficient for some indicators of OPC fate (Table S1), oligodendrocyte differentiation was not observed from infected NPCs after growth factor removal. The principal effect of ASCL1 overexpression was induction of a neuronal-like morphology and βIII-tubulin expression. Interestingly, transient expression was also sufficient to induce NG2 expression, but did not lead to oligodendrocyte differentiation after growth factor removal. As observed with constitutive expression, transient ASCL1 overexpression induced neuronal-like differentiation. Although OLIG2 was repressed in ASCL1-infected NPCs, thereby possibly limiting differentiation, concurrent infection with ASCL1 and OLIG2 did not induce oligodendrocyte differentiation. This suggests that the absence of oligodendrocyte differentiation following ASCL1 or PRRX1 overexpression is related not to direct inhibition of differentiation, but rather to the lack of another factor (possibly SOX10) that limits the differentiation capacity of induced OPCs. Thus, additional work is needed to precisely define the combinations, timing, and posttranscriptional regulation of these factors to increase the efficiency of OPC fate.

Somatic cell reprogramming through various combinations of TF overexpression has been established as a novel means to induce transdifferentiation of various somatic cell types, typically fibroblasts, to neuronal and other lineages (39). Two recent studies have demonstrated this approach with rodent fibroblasts and induction of OPC-like and oligodendrocyte fate using a combination of Sox10, Olig2, and either Zfp546 or Nkx6.2 (40, 41); however, neither of these approaches has been

successful thus far in human fibroblasts. Given the transcriptional differences between mouse and human OPCs (14), the specific factors sufficient to induce OPCs from human cells likely are different. Indeed, when we examined which genes were activated by SOX10 in human NPCs, we found no significant enrichment relative to known rodent target genes [receiver operating characteristic (ROC)-based area under the curve analysis] (30). These data suggest that the precise effect of each overexpressed TF may differ based on species and cellular environment.

In summary, we found that directly targeting SOX10 expression in human NPCs promoted OPC specification, oligodendrocyte differentiation, and myelination of transplanted human progenitor cells. These data suggest that SOX10 is one of the principle gatekeepers for oligodendrocyte lineage fate. Thus, small molecules or cell signaling cascades that induce SOX10 expression might be expected to enhance OPC specification and myelination by both endogenous and transplanted human cells. Because cells derived from pluripotent stem cells transition through the same developmental stages, we hypothesize that agents capable of inducing SOX10 expression and precocious myelination likely would be similarly effective and useful as adjuncts to iPSC-based approaches. Alternatively, by identifying the key targets of SOX10 that drive oligodendrocyte differentiation, we may be able to similarly promote differentiation and myelination in a variety of neurologic diseases without directly targeting SOX10.

Materials and Methods

Tissue Samples. Fetal brain samples at 15–22 wk gestational age were obtained from patients who consented to tissue use under protocols approved by the local Institutional Review Board. Dissociates were prepared as described previously (42) and cultured in serum-free medium (SFM) as detailed previously (5) with 10 ng/mL FGF2 (PeproTech).

Cytometry/FACS. Cytometry and sorting were performed with a BD FACSAria cell sorter, as described previously (15). For CD133/CD140a, cells were stained with CD140a-PE (BD Pharmingen) and CD133-APC (Miltenyi Biotech). Matched fluorescence minus-one controls were used to set gates following doublet discrimination.

qPCR Analyses. Immediately after CD133/CD140a FACS, RNA extraction, first-strand synthesis, and qPCR were performed, as described previously (16). Human primers for SYBR Green-based PCR and predesigned primer and Taqman probes were purchased from IDT and Invitrogen, respectively (Table S2). Samples were run in duplicate, and gene expression was calculated by ΔΔCt analysis using GAPDH as a reference. GAPDH was chosen following initial experiments that used 18S rRNA as a reference gene. Because both reference genes showed very high correlation ($R^2 = 0.91$), we used GAPDH in all subsequent experiments.

To determine the effect of TF overexpression of OPC-specific gene expression, we plated $CD133^+CD140a^-$ NPCs onto polyornithine/laminin substrate and infected them the next day with lentivirus. Cells were maintained in SFM with either 20 ng/mL EGF and 20 ng/mL FGF-2 or 20 ng/mL PDGF-AA and 5 ng/mL FGF-2 before extraction and qPCR analysis 7 d later.

TF and Lentiviral Cloning. We cloned the coding regions of each identified factor into a lentiviral backbone derived from pTRIP-EF1a (43) (a gift from Abdel Benraiss, University of Rochester, Rochester, NY). In brief, human TF coding sequences (CDSs) were obtained either from existing plasmids or reverse-transcribed human cDNA and then PCR-cloned into pCR2.1 TOPO4 plasmid (Life Technologies). The CDS was then transferred into pTRIP-EF1α by replacing mCherry using unique restriction sites (Table S3). Lentiviruses were prepared as described previously (44). In brief, after triple transfection of HEK 293T cells with pTRIP and packaging plasmids pLP/VSVG (Life Technologies) and psPAX2 (AddGene), viral supernatant was collected at 48 and 72 h. Titration of virus was performed on matched mCherry-expressing virus using flow cytometry for mCherry fluorescence and directly compared with TF viruses using qPCR for the WPRE sequence (45). Confirmation of TF expression was performed after infection in 293T cells (Table S3). Human primary cells were infected at 1 multiplicity of infection (MOI) for 24 h, followed by complete medium replacement unless stated otherwise.

Sox10-MCS5:GFP Reporter. Following FACS, cells were plated at 5×10^4/mL on polyornithine/laminin-coated plates in SFM with EGF/FGF2 (20 ng/mL; PeproTech). On the next day, cells were infected with Sox10-MCS5:GFP reporter lentivirus at 1 MOI (18). Virus carrying individual TFs was added to cell culture at 1 MOI 24 h after SOX10-MCS5:GFP virus infection. Cytometry was performed 4 d thereafter. Cells were gated using FSC/SSC, and GFP expression was measured.

In Vitro Immunostaining. Following FACS, human $CD133^+CD140a^-$ NPCs were plated at 5×10^4/mL on polyornithine/laminin-coated 24-well plates in SFM supplemented with 20 ng/mL EGF/FGF2. At 24 h later, cells were infected with lentivirus at 1 MOI. For assessment of OPC induction, cells were live stained with A2B5 (1:1, hybridoma supernatant; American Type Culture Collection) or fixed for NG2 (mouse IgG2a, 1:200; Millipore). For oligodendrocyte differentiation, cells were further maintained in SFM supplemented with 20 ng/mL PDGF and 5 ng/mL FGF2 for 6 d, followed by 5 ng/mL NT-3 until day 14 or 21. Cells were immunostained for OLIG2/O4 as described previously (16), or with MBP (rat IgG, 1:200; Abcam). Alexa Fluor 594-, 647-, and 488-conjugated goat secondary antibodies (Life Technologies) were used at 1:500 dilution. In all experiments, uninfected human $CD140a^+$ OPCs were maintained in the same conditions as positive controls. For cell counting, at least 200 live cells were counted from five randomly selected fields (20×) or >500 cells along the diameter of the well.

Microarray Analysis. Human $CD133^+CD140a^-$ NPCs were infected with individual TFs or mCherry-expressing lentivirus at 24 h post-FACS. Infected cells were maintained in mitotic conditions containing EGF/FGF for another 7 d before RNA extraction. To determine the expression profile of infected cells, we performed Illumina microarray analysis ($n = 2$ fetal samples) and combined these data with the expression profile of CD133/CD140a sorted cells ($n = 3$ fetal samples) (15). RNA was amplified and Illumina HT-12v4 bead arrays analysis was performed using R/Bioconductor, as described previously (16). We identified genes as significantly regulated using a moderated t test statistic ($P < 0.01$) and further filtered these genes to examine only those regulated by two or more. Gene set enrichment analysis was performed (46) using a custom gene set collection compiled from human CD140a/O4 (16), CD133/CD140a (15), and mouse immunopanned cells (19). ROC-based area under the curve data and significance of gene set enrichment were calculated using roc.area (47). TF-infected cell populations were compared using roc.test (48).

Transplantation into *shiverer/rag2* Mice. ***Animals and Surgery.*** All experiments using *shiverer/rag2* mice (a gift of Dr. Steven A. Goldman, University of Rochester, Rochester, NY) (3) were performed according to protocols approved by the University at Buffalo's Institutional Animal Care and Use Committee. If necessary, newborn pups were genotyped on the day of birth to identify homozygote *shiverer* mice. Human NPCs and OPCs were cultured for up to 1 wk in SFM containing EGF/FGF and PDGF/FGF, respectively, and frozen using ProFreeze (Lonza) before surgery. At 24 h after thawing, cells were infected with lentivirus at 1 MOI and then allowed to recover for 1–2 d before surgery. Cells were prepared for injection by resuspending cells in HBSS(−) at 1×10^5 cells/μL. Injections were performed as described previously (5). In brief, pups were anesthetized using hypothermia, and 5×10^4 cells were injected in each site, bilaterally, at a depth of 1.1 mm into the corpus callosum of postnatal day 2–3 pups. Cells were injected through pulled glass pipettes inserted directly through the skull into the presumptive target sites. Animals were killed and perfused with saline, followed by 4% paraformaldehyde, at 8 or 12 wk.

In Vitro Analysis. As a quality control for the cells used for implantation, the remaining postimplantation cells were plated onto polyornithine/laminin-coated plates and analyzed on day 1 or 14. On day 1, NPCs were assessed for mCherry expression, and neural progenitor fate was assessed by immunostaining for nestin (1:1,000; Millipore). On day 14, cells were stained with O4 to detect oligodendrocyte differentiation in vitro. Almost all (>95%) of the cells prepared for transplantation remained nestin-expressing NPCs at 1 d after injection, and >90% of cells expressed mCherry, indicating efficient viral transduction.

In Vivo Immunostaining. Cryopreserved coronal sections of mouse forebrain (16 μm) were cut, and brains were sampled every 160 μm. Immunohistochemistry was performed as described previously (5). Human cells were identified with mouse anti-human nuclei (mouse IgG1, 1:100, clone 235–1; Millipore), and myelin basic protein-expressing oligodendrocytes were labeled with MBP. Oligodendrocytes, human astrocytes, human OPCs, and human NPCs were recognized by CC1 (mouse IgG2b, 1:50; EMD Chemicals), hGFAP (mouse IgG1, 1:800; Covance), hNG2 (mouse IgG2a, 1:800; Millipore), and hNestin

(mouse IgG1, 1:1000; Millipore), respectively. Mouse neurofilament (NF) was stained with a 1:1 mixture of SMI311 and SMI312 (mouse IgG1, 1:800; Covance). Alexa Fluor secondary antibodies, goat anti-mouse 488, rat 594, and rabbit 647 (Life Technologies), were used at 1:500.

Microscopy. To quantify the proportion of MBP^+ oligodendrocytes in the fimbria, we sampled four sections at random from every 160 μm with a 40× objective in each animal. Between 500 and 1,000 hNA^+MBP^+ cells were counted for each animal. The proportion of mCherry- and HA-expressing MBP^+ cells was assessed in a similar manner. For assessment of human $CC1^+$ oligodendrocyte differentiation in the corpus callosum, mosaic pictures of four sections encompassing the corpus callosum were captured using Zeiss Axiovision software with a 10× objective. $CC1^+/hNA^+$ cells were quantified by counting cells in midline and lateral regions in the corpus callous; more than 1,500 cells per animal were counted. MBP ensheathment of host axons was assessed in the corpus callosum as described previously (3). In brief, a 2-μm stack of 20 optical sections was obtained every 0.1 μm, and the proportion of ensheathed axons that crossed three perpendicular sampling lines placed randomly over each image was counted (Zeiss LSM 510 Meta NLO confocal microscope).

ACKNOWLEDGMENTS. We thank Dr. J. Conroy of Roswell Park Cancer Institute (RPCI) for assistance with the Illumina bead array techniques. We acknowledge the assistance of the Confocal Microscope and Flow Cytometry Facility in the School of Medicine and Biomedical Sciences, University at Buffalo. We also thank Dr. K. Morrison of the Buffalo Womenservices clinic and Dr. B. Poulos of the Human Fetal Tissue Repository at the Albert Einstein College of Medicine for assistance with tissue acquisition, and L. Lin and J. Noble for technical assistance. This work was supported in part by the Empire State Stem Cell Fund through New York State Department of Health Contracts C026413 and C028108. The microarray profiling was supported by grants from the National Institutes of Health/National Cancer Institute (RPCI Cancer Center Support Grant P30 CA016056).

1. Goldman SA, Nedergaard M, Windrem MS (2012) Glial progenitor cell-based treatment and modeling of neurological disease. *Science* 338(6106):491–495.
2. Franklin RJ, French-Constant C (2008) Remyelination in the CNS: From biology to therapy. *Nat Rev Neurosci* 9(11):839–855.
3. Windrem MS, et al. (2008) Neonatal chimerization with human glial progenitor cells can both remyelinate and rescue the otherwise lethally hypomyelinated shiverer mouse. *Cell Stem Cell* 2(6):553–565.
4. Windrem MS, et al. (2004) Fetal and adult human oligodendrocyte progenitor cell isolates myelinate the congenitally dysmyelinated brain. *Nat Med* 10(1):93–97.
5. Sim FJ, et al. (2011) CD140a identifies a population of highly myelinogenic, migration-competent and efficiently engrafting human oligodendrocyte progenitor cells. *Nat Biotechnol* 29(10):934–941.
6. Uchida N, et al. (2012) Human neural stem cells induce functional myelination in mice with severe dysmyelination. *Sci Transl Med* 4(155):155ra136.
7. Hu BY, Du ZW, Zhang SC (2009) Differentiation of human oligodendrocytes from pluripotent stem cells. *Nat Protoc* 4(11):1614–1622.
8. Izrael M, et al. (2007) Human oligodendrocytes derived from embryonic stem cells: Effect of noggin on phenotypic differentiation in vitro and on myelination in vivo. *Mol Cell Neurosci* 34(3):310–323.
9. Hu BY, Du ZW, Li XJ, Ayala M, Zhang SC (2009) Human oligodendrocytes from embryonic stem cells: Conserved SHH signaling networks and divergent FGF effects. *Development* 136(9):1443–1452.
10. Wang S, et al. (2013) Human iPSC-derived oligodendrocyte progenitor cells can myelinate and rescue a mouse model of congenital hypomyelination. *Cell Stem Cell* 12(2):252–264.
11. Chandran S, et al. (2004) Differential generation of oligodendrocytes from human and rodent embryonic spinal cord neural precursors. *Glia* 47(4):314–324.
12. Zhang SC, Ge B, Duncan ID (2000) Tracing human oligodendroglial development in vitro. *J Neurosci Res* 59(3):421–429.
13. Emery B (2010) Regulation of oligodendrocyte differentiation and myelination. *Science* 330(6005):779–782.
14. Sim FJ, Windrem MS, Goldman SA (2009) Fate determination of adult human glial progenitor cells. *Neuron Glia Biol* 5(3-4):45–55.
15. Wang J, O'Bara MA, Pol SU, Sim FJ (2013) CD133/CD140a-based isolation of distinct human multipotent neural progenitor cells and oligodendrocyte progenitor cells. *Stem Cells Dev* 22(15):2121–2131.
16. Conway GD, O'Bara MA, Vedia BH, Pol SU, Sim FJ (2012) Histone deacetylase activity is required for human oligodendrocyte progenitor differentiation. *Glia* 60(12):1944–1953.
17. Sugimori M, et al. (2008) Ascl1 is required for oligodendrocyte development in the spinal cord. *Development* 135(7):1271–1281.
18. Pol SU, et al. (2013) Sox10-MCS5 enhancer dynamically tracks human oligodendrocyte progenitor fate. *Exp Neurol* 247:694–702.
19. Cahoy JD, et al. (2008) A transcriptome database for astrocytes, neurons, and oligodendrocytes: A new resource for understanding brain development and function. *J Neurosci* 28(1):264–278.
20. Furusho M, et al. (2006) Involvement of the Olig2 transcription factor in cholinergic neuron development of the basal forebrain. *Dev Biol* 293(2):348–357.
21. Lu QR, et al. (2002) Common developmental requirement for Olig function indicates a motor neuron/oligodendrocyte connection. *Cell* 109(1):75–86.
22. McClain CR, Sim FJ, Goldman SA (2012) Pleiotrophin suppression of receptor protein tyrosine phosphatase-β/ζ maintains the self-renewal competence of fetal human oligodendrocyte progenitor cells. *J Neurosci* 32(43):15066–15075.
23. Fancy SP, Chan JR, Baranzini SE, Franklin RJ, Rowitch DH (2011) Myelin regeneration: A recapitulation of development? *Annu Rev Neurosci* 34:21–43.
24. Gobert RP, et al. (2009) Convergent functional genomics of oligodendrocyte differentiation identifies multiple autoinhibitory signaling circuits. *Mol Cell Biol* 29(6):1538–1553.
25. Shimozaki K, Clemenson GD, Jr, Gage FH (2013) Paired related homeobox protein 1 is a regulator of stemness in adult neural stem/progenitor cells. *J Neurosci* 33(9):4066–4075.
26. Zhang D, et al. (2006) Identification of potential target genes for RFX4_v3, a transcription factor critical for brain development. *J Neurochem* 98(3):860–875.
27. Ming X, Chew LJ, Gallo V (2013) Transgenic overexpression of Sox17 promotes oligodendrocyte development and attenuates demyelination. *J Neurosci* 33(30):12528–12542.
28. Maire CL, Wegener A, Kerninon C, Nait Oumesmar B (2010) Gain-of-function of Olig transcription factors enhances oligodendrogenesis and myelination. *Stem Cells* 28(9):1611–1622.
29. Liu Z, et al. (2007) Induction of oligodendrocyte differentiation by Olig2 and Sox10: Evidence for reciprocal interactions and dosage-dependent mechanisms. *Dev Biol* 302(2):683–693.
30. Pozniak CD, et al. (2010) Sox10 directs neural stem cells toward the oligodendrocyte lineage by decreasing Suppressor of Fused expression. *Proc Natl Acad Sci USA* 107(50):21795–21800.
31. Lu QR, et al. (2000) Sonic hedgehog—regulated oligodendrocyte lineage genes encoding bHLH proteins in the mammalian central nervous system. *Neuron* 25(2):317–329.
32. Lu QR, Cai L, Rowitch D, Cepko CL, Stiles CD (2001) Ectopic expression of Olig1 promotes oligodendrocyte formation and reduces neuronal survival in developing mouse cortex. *Nat Neurosci* 4(10):973–974.
33. Copray S, et al. (2006) Olig2 overexpression induces the in vitro differentiation of neural stem cells into mature oligodendrocytes. *Stem Cells* 24(4):1001–1010.
34. Jessberger S, Toni N, Clemenson GD, Jr, Ray J, Gage FH (2008) Directed differentiation of hippocampal stem/progenitor cells in the adult brain. *Nat Neurosci* 11(8):888–893.
35. Maire CL, et al. (2009) Directing human neural stem/precursor cells into oligodendrocytes by overexpression of Olig2 transcription factor. *J Neurosci Res* 87(15):3438–3446.
36. Zhou Q, Wang S, Anderson DJ (2000) Identification of a novel family of oligodendrocyte lineage-specific basic helix-loop-helix transcription factors. *Neuron* 25(2):331–343.
37. Küspert M, Hammer A, Bösl MR, Wegner M (2011) Olig2 regulates Sox10 expression in oligodendrocyte precursors through an evolutionary conserved distal enhancer. *Nucleic Acids Res* 39(4):1280–1293.
38. Li H, de Faria JP, Andrew P, Nitarska J, Richardson WD (2011) Phosphorylation regulates OLIG2 cofactor choice and the motor neuron-oligodendrocyte fate switch. *Neuron* 69(5):918–929.
39. Vierbuchen T, Wernig M (2012) Molecular roadblocks for cellular reprogramming. *Mol Cell* 47(6):827–838.
40. Najm FJ, et al. (2013) Transcription factor-mediated reprogramming of fibroblasts to expandable, myelinogenic oligodendrocyte progenitor cells. *Nat Biotechnol* 31(5):426–433.
41. Yang N, et al. (2013) Generation of oligodendroglial cells by direct lineage conversion. *Nat Biotechnol* 31(5):434–439.
42. Windrem MS, et al. (2002) Progenitor cells derived from the adult human subcortical white matter disperse and differentiate as oligodendrocytes within demyelinated lesions of the rat brain. *J Neurosci Res* 69(6):966–975.
43. Sevin C, et al. (2006) Intracerebral adeno-associated virus-mediated gene transfer in rapidly progressive forms of metachromatic leukodystrophy. *Hum Mol Genet* 15(1):53–64.
44. Sim FJ, et al. (2006) Complementary patterns of gene expression by human oligodendrocyte progenitors and their environment predict determinants of progenitor maintenance and differentiation. *Ann Neurol* 59(5):763–779.
45. Geraerts M, Willems S, Baekelandt V, Debyser Z, Gijsbers R (2006) Comparison of lentiviral vector titration methods. *BMC Biotechnol* 6:34.
46. Furge KA, et al. (2007) Identification of deregulated oncogenic pathways in renal cell carcinoma: An integrated oncogenomic approach based on gene expression profiling. *Oncogene* 26(9):1346–1350.
47. Mason SJ, Graham NE (2002) Areas beneath the relative operating characteristics (ROC) and relative operating levels (ROL) curves: Statistical significance and interpretation. *Q J R Meteorol Soc* 128(584):2145–2166.
48. DeLong ER, DeLong DM, Clarke-Pearson DL (1988) Comparing the areas under two or more correlated receiver operating characteristic curves: A nonparametric approach. *Biometrics* 44(3):837–845.